4-12-2005

Fire Retardancy of Polystyrene - Hectorite Nanocomposites

Dongyan Wang
Marquette University

Bok Nam Jang
Marquette University

Shengpei Su
Marquette University

Jinguo Zhang
Marquette University

Xiaoxia Zheng
Marquette University

See next page for additional authors

Published version. Published as a chapter of a book entitled *Fire Retardancy of Polymers: New Applications of Mineral Fillers*. Eds. Michel Le Bras, Serge Bourbigot, Sophie Duquesne, Charafedine Jama, Charles Wilkie. Cambridge, UK: Royal Society of Chemistry, 2005, pp. 126-138, DOI: 10.1039/9781847552396-00126.

CHAPTER 9

Fire Retardancy of Polystyrene –Hectorite Nanocomposites

DONGYAN WANG, BOK NAM JANG, SHENGPEI SU, JINGUO ZHANG, XIAOXIA ZHENG, GRACE CHIGWADA, DAVID D. JIANG AND CHARLES A. WILKIE

Department of Chemistry, Marquette University, PO Box 1881, Milwaukee, WI 53201, U.S.A. (charles.wilkie@marquette.edu)

9.1 Introduction

Polymer nanocomposites have become an area of extensive research in recent years. The properties of polymer nanocomposite are expected to be improved significantly in the presence of layered silicate materials.[1–6] Amongst these layered silicate materials, montmorillonite is the most popular one studied, but some attention has also been paid to magadiite,[7–12] bentonite[13–16] and hectorite.[17–22]

While montmorillonite is an aluminosilicate, magadiite and hectorite contain only silicates. The chemical formula for hectorite is $Na_{0.3}(Mg,Li)_3Si_4O_{10}(OH)_2$; a specimen of hectorite, fresh from the mine, has a soft, greasy texture; it is one of the more expensive clays, due to its unique thixotropic properties. The major uses of hectorite are in cosmetics and in chemical and industrial material production.

Polyolefin microcomposites and layered silicate nanocomposites have been prepared by Dubois *et al.*[17] *via in situ* polymerization, using both montmorillonite and hectorite that had been treated with trimethylaluminum-depleted methylaluminoxane. The encapsulated filler particle within the (co)polyolefinic matrix formed polymers ranging from thermoplastics to elastomers. The obtained "homogeneous" (nano)composites exhibit improved mechanical properties, as compared to more conventional melt blends for the same filler content. Sandi[18] has synthesized a series of polymer–clay nanocomposites based on synthetic lithium hectorite and different mass ratios of poly(ethylene oxide) and tested these as candidates for polymeric electrolytes in lithium ion cells.

Transparent films with excellent mechanical strength were obtained with a conductivity that is comparable to more traditional polymer electrolytes made with added lithium salts.

Coumarin dye molecules were first intercalated into the gallery of hectorite; extensive shaking and sonication of this water suspension leads to exfoliation, which is confirmed by both atomic force microscopy (AFM) and transmission electron microscopy (TEM).[19] The resulting nanocomposite films were transparent and displayed fluorescence centered at around 470 nm.

Polystyrene–clay and poly(methyl methacrylate)–clay nanocomposites[20] have been prepared using cetyltrimethylammonium-modified hectorite by solution blending in toluene. Wide-angle X-ray diffraction (WAXD) as well as 2D ^{1}H–^{29}Si and ^{1}H–^{1}H correlated solid-state NMR confirmed the dispersion of the intercalated clay stacks in the polymer matrix.

Multinuclear solid-state NMR (two-dimensional ^{1}H–^{29}Si heteronuclear correlation (HETCOR) NMR with spin diffusion and refocused ^{29}Si detection for enhanced sensitivity) revealed that during the intercalation of poly(styrene-ethylene oxide) block copolymers (PS-b-PEO) into hectorite, the PS block is not intercalated but the PEO segment is intercalated.[21] In PS-rich samples, a small amount of PEO is intercalated and a significant fraction of PEO is not intercalated. Intercalated PEO exhibits reduced mobility, most prominently for the PEO nearest to the silicate surface. *In situ* small-angle X-ray scattering studies were conducted to monitor the structural changes of polymer nanocomposites upon heating.[22]

These silicates usually have excess negative charge, which is balanced by the exchangeable cations in the gallery space. Like montmorillonite clay, the cation exchangeability offers the possibility for the modification of pristine hectorite by organic cations, which can increase the organophilic character of the gallery space so that it is compatible with an organic polymer. Because of the outstanding performance of montmorillonite clay in the enhancement of barrier properties and in fire retardancy, there is interest in examining hectorite, and other clays, to determine how different clays behave with respect to nanocomposite formation and in fire performance.

In this chapter, pristine hectorite was modified with two different quaternary ammonium salts, one of which is known to give intercalated and the other to give exfoliated nanocomposites with montmorillonite, and polystyrene nanocomposites were prepared by bulk polymerization.

9.2 Experimental

9.2.1 Materials

Dimethylhexadecylamine (≥98%) was acquired from Fluka. Most of the other chemicals used in this study, including vinylbenzyl chloride (97%), monomeric styrene, benzoyl peroxide (BPO) 97% and tetrahydrofuran (THF) (99+%), were purchased from the Aldrich Chemical Company. The polymerization inhibitor was removed from the monomer by passing it through an inhibitor-remover

column, also acquired from Aldrich. The quaternary ammonium salt known as 10A was kindly provided by Akzo-Nobel, while the salt known as VB was synthesized in this laboratory following a previously published procedure.[23] Distilled water was used throughout as needed. Hectorite slurries were kindly provided by Elementis Specialties, Inc.; the iron contents of the clays and the lot numbers by which they are reported herein are: 66A, 0.053%; 66B, 0.53%; and 66G, 2.57%.

9.2.2 Organic Modification of Hectorite

The method used for the organic-modification of hectorite was quite similar to that used to modify montmorillonite clay, as reported previously.[24] The cationic exchange reaction occurs between pristine hectorite and a quaternary ammonium salt, in this case styryldimethylhexadecylammonium chloride (VB16, denoted VB) and dimethylbenzylhydrogenated tallow chloride (10A) were utilized. Hydrogenated tallow contains ~65% C18, ~30% C16 and ~5% C14. A 10% mole excess of the quaternary ammonium salt (based on the CEC of the hectorite) was added to the hectorite slurry for the cationic exchange reaction. After overnight stirring, the reaction was stopped, then the organically-modified hectorite was dried in a vacuum oven at room temperature.

9.2.3 Preparation of Nanocomposites

A bulk polymerization technique was utilized in the preparation of the polystyrene (PS) hectorite nanocomposite. This procedure, which has been used for montmorillonite, has been previously described.[24]

9.2.4 Instrumentation

X-Ray diffraction (XRD) patterns were obtained using a Rigaku Geiger Flex, 2-circle powder diffractometer equipped with Cu Kα generator ($\lambda = 1.5404$ Å). Generator tension was 50 kV and generator current was 20 mA.

Thermogravimetric analysis (TGA) was performed on a TA Instruments, model SDT 2960 Simultaneous DTA-TGA unit under a 40 mL min^{-1} flowing nitrogen atmosphere at a scan rate of 10°C min^{-1} from room temperature to 700°C; temperatures are reproducible to ±3°C, and the fraction of nonvolatile materials is reproducible to ±3%.

Cone calorimetry was performed on an Atlas CONE2 according to ASTM E 1354-92 at an incident flux of 35 kW m^{-2} using a cone shaped heater. Exhaust flow was set at 24 L s^{-1} and the spark was continuous until the sample ignited. Cone samples were prepared by compression molding the sample (about 30 g) into square plaques. Typical results from Cone calorimetry are reproducible to within about ±10%. These uncertainties are based on many runs in which thousands of samples have been combusted.[25]

9.3 Results and Discussions

9.3.1 X-ray Diffraction

XRD can provide information about the *d*-spacing of hectorite according to the Bragg equation. The *d*-spacing of pristine hectorite is 1.1 nm ($2\theta = 7.9°$); after organic-modification with the 10A salt, the *d*-spacing increased to 2.0 nm ($2\theta = 4.4°$), indicating that ion-exchange occurred. After bulk polymerization of styrene with the clay, the XRD trace shows a sharp, strong peak at about 3.5 nm ($2\theta = 2.5°$), clearly indicating the formation of an intercalated nanocomposite; XRD traces for the PS-hectorite 10A nanocomposites are shown in Figure 1.

For the VB system, the *d*-spacing after ion exchange is also at 2.0 nm ($2\theta = 4.4°$). Peaks in the XRD traces (Figure 2) are much weaker for the VB system than for the 10A system. This may be attributable to either a greater extent of exfoliation or disorder of the clay and an immiscible system. This last possibility is rejected because VB invariably gives better exfoliation than does a non-functionalized organic-modification such as 10A.[23]

Identical results were obtained for all of the hectorites examined in this study. There is little doubt, based on the XRD results, that these are intercalated and exfoliated nanocomposites.

9.3.2 Transmission Electron Microscopy

The XRD results very strongly suggest that good nanodispersion has been achieved for all of these nanocomposites, but the only proof of this assertion lies

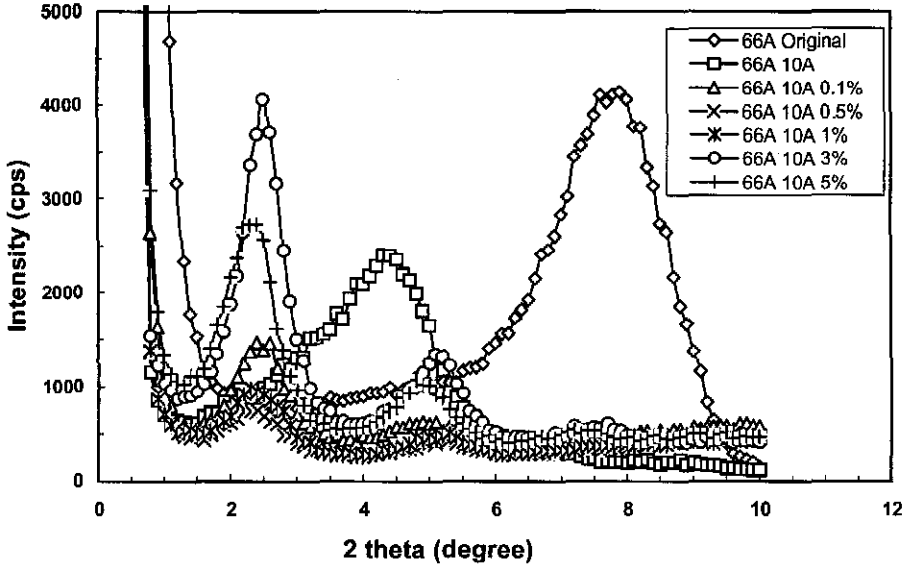

Figure 1 *XRD traces for PS-hectorite 10A systems*

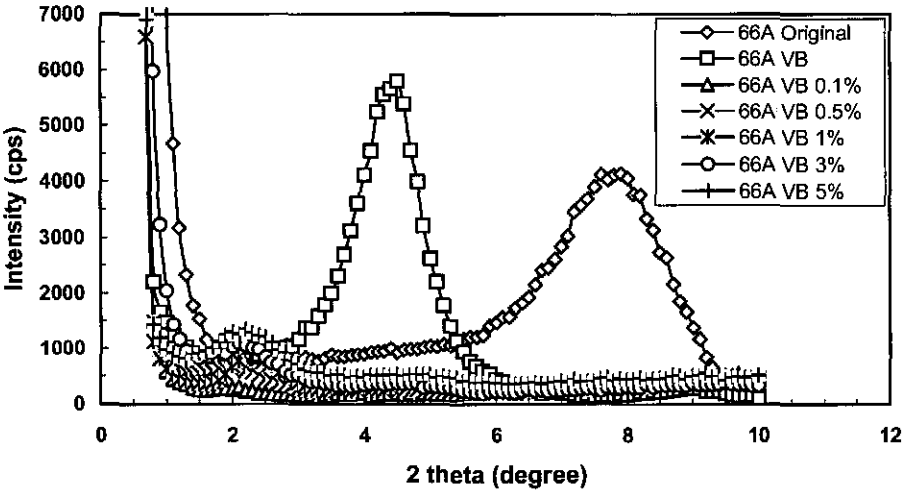

Figure 2 *XRD traces for PS-hectorite VB systems*

in TEM data. TEM images at both low and high magnification for the VB-PS nanocomposites are shown in Figure 3 while those for the 10A-PS system are shown in Figure 4. For both systems one can see that good nanodispersion has been obtained and the high magnification images enable one to see the individual clay layers and to specify that the VB system is more exfoliated than is the 10A system.

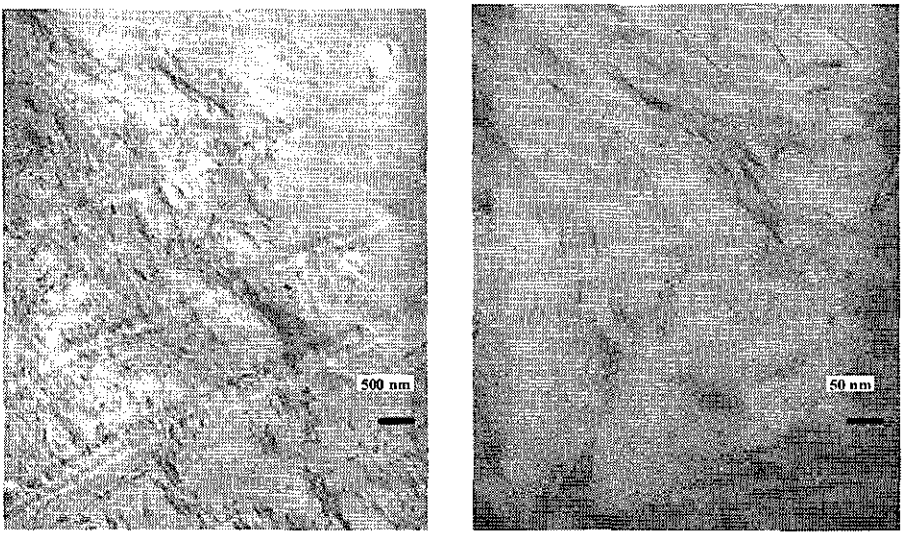

Figure 3 *TEM images at low magnification (left) and high magnification (right) for the VB-PS nanocomposite*

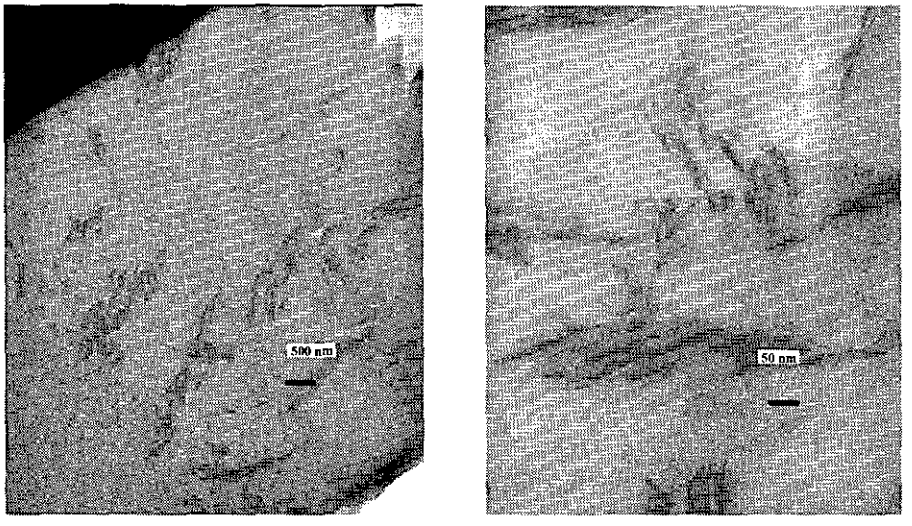

Figure 4 *TEM images at low (left) and high magnification (right) for the 10A-PS nanocomposite*

9.3.3 Thermogravimetric Analysis

Parameters extracted from the TGA include the temperature at which 10% of the mass has been lost, $T_{0.1}$, a measure of the onset of degradation, the temperature at which 50% of the mass is lost, $T_{0.5}$, the mid-point of the degradation, and the fraction of material that is not volatile at 600°C (denoted as char). With montmorillonite clays we found previously that the onset temperature, as well as the mid-point temperature, of iron-containing clay increases by about 50°C compared to virgin polymer.[26] Results for the hectorite clay systems (Table 1) show comparable results for both temperatures; a representative set of TGA curves for one of these systems is shown in Figure 5.

There appears to be some difference between lower amounts of clay and the results at 3 or 5%, especially for the mid-point of the degradation, with larger increases in temperature at these clay levels. With the montmorillonite, if one compared iron-containing with iron-free clays, there was a significant temperature difference between the two clays at low amounts of clay, but this difference became smaller as the amount of clay increased and became negligible at 3 or 5% clay. With hectorite, there is no difference that can be attributed to the presence or absence of iron. The tentative conclusion is that hectorite and montmorillonite exhibit similar effects according to TGA analysis, but the amount of iron is important for montmorillonite but not for hectorite.

9.3.4 Cone Calorimetry

Cone calorimetry enables the evaluation of the fire parameters for a system; the data that may be obtained includes the heat release rate curve, the total heat

Table 1 *TGA parameters for hectorite-PS nanocomposites*

Sample	$T_{0.1}$ (°C)	$T_{0.5}$ (°C)	*Char* (wt%)
PS	351	404	0
66A-10A-PS, 0.1%	382	425	0
66A-10A-PS, 0.5%	399	436	0
66A-10A-PS, 1%	392	435	0
66A-10A-PS, 3%	390	444	2
66A-10A-PS, 5%	389	446	3
66A-VB-PS, 0.1%	387	428	0
66A-VB-PS, 0.5%	391	427	0
66A-VB-PS, 1%	399	436	0
66A-VB-PS, 3%	389	428	1
66A-VB-PS, 5%	414	457	5
66B-10A-PS, 0.1%	365	417	0
66B-10A-PS, 0.5%	380	426	0
66B-10A-PS, 1%	404	437	0
66B-10A-PS, 3%	389	443	3
66B-10A-PS, 5%	399	448	3
66B-VB-PS, 0.1%	337	402	0
66B-VB-PS, 0.5%	356	410	0
66B-VB-PS, 1%	364	422	2
66B-VB-PS, 3%	404	445	2
66B-VB-PS, 5%	408	452	5
66G-10A-PS, 0.1%	382	424	0
66G-10A-PS, 0.5%	403	436	0
66G-10A-PS, 1%	400	440	1
66G-10A-PS, 3%	400	444	3
66G-VB-PS, 0.1%	383	421	0
66G-VB-PS, 0.5%	394	421	0
66G-VB-PS, 1%	393	425	0
66G-VB-PS, 3%	400	445	2

released, mass loss rate, time to ignition and smoke evolution, known as the specific extinction area. For montmorillonite-polystyrene nanocomposites, the time to ignition is decreased, the total heat released is unchanged but the peak heat release rate, PHRR, is significantly decreased, typically by 50–60%, the mass loss rate is also reduced and there is little change in smoke evolution. In a study of iron-containing versus iron-free polystyrene-montmorillonite nanocomposites, we found a significant difference in the PHRR for iron-containing clays at low amounts of clay, but this difference vanishes as the amount of clay increases.[26] The commonly accepted mechanism by which nanocomposite formation reduces the PHRR is through barrier formation, which can act both as an insulator and a barrier to mass transport.[27] Based upon these observations on the effect of iron, it was proposed that some radical trapping may occur and that this is an effective mechanism at low clay content but, at high clay content, the barrier effect becomes dominant.

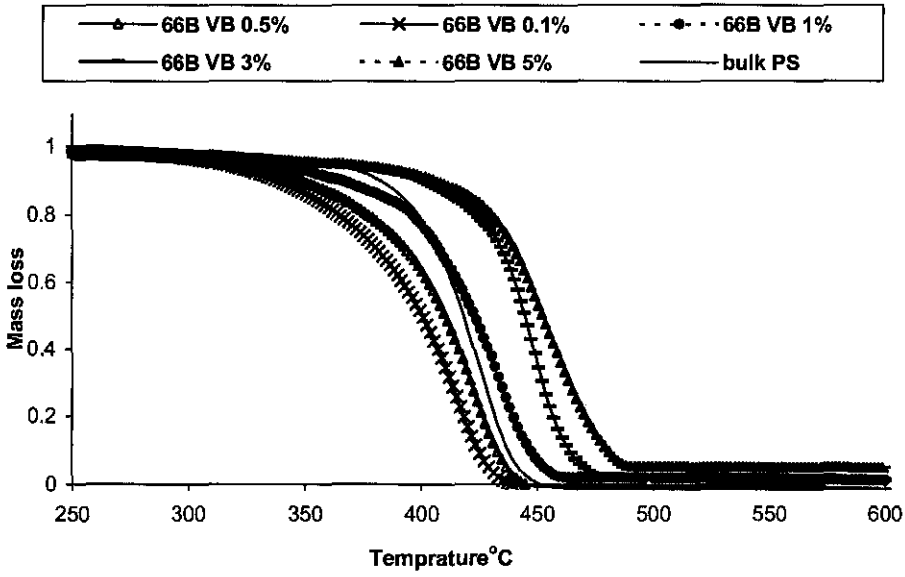

Figure 5 *TGA curves for 66B-VB-PS nanocomposites*

For hectorite-polystyrene nanocomposites the results are quite different; the cone calorimetric results are shown in Table 2, while Figure 6 shows a representative plot of the heat release rate for one of the polystyrene-hectorite nanocomposites. There is essentially no reduction in PHRR when the clay content is 1% or less and in some cases there is no effect at 3% clay, an amount at which montmorillonite is very effective. In most cases, at 5% clay one sees a reasonable reduction in PHRR. The other parameters recorded in Table 2 are typical values and confirm the PHRR observation. For instance, when there is no reduction in PHRR, there is also no change in mass loss rate.

One can examine the data as a function of morphology, the 10A series *versus* the VB series, or as a function of iron content. From the XRD traces, those nanocomposites made with the 10A salt show a peak and are presumed to be intercalated while those made with VB16 show no peak and thus are assumed to be exfoliated; the TEM data confirms these suggestions. For the very low iron content clay, 66A, the one discontinuity appears at 3% clay where the intercalated material, 10A, gives a reduction while the exfoliated VB system gives no reduction.

For the intermediate iron content clay, 66B, a similar trend is seen in which the intercalated system gives a slight reduction at low amounts of clay and there is a major difference at 3% clay. This trend is not continued at higher amounts of iron, 66G; here there is no reduction for the intercalated system but a better reduction for the exfoliated system. These discrepancies cannot be attributed to changes in the dispersion of the clay within the polymer matrix and must be due to something else.

Table 2 *Cone calorimetric data for the hectorite-polystyrene nanocomposites*

Sample	T_p (s)	*PHRR* (kW m^{-2})	*THR* (mJ m^{-2})	*WLR,* (g s^{-1} m^{-2})	SEA_{av} (g s^{-1} m^{-2})
Polystyrene	59	1200	89	31.7	952
66A-10A-PS, 0.1%	58	1149(4)	94	27.8	1138
66A-10A-PS, 0.5%	60	1223(0)	98	29.8	1117
66A-10A-PS, 1%	62	1440(0)	120	29.8	1342
66A-10A-PS, 3%	51	634 (31)	91	20.8	1285
66A-10A-PS, 5%	59	771 (36)	94	20.1	1322
66A-VB-PS, 0.1%	54	1505 (0)	112	29.2	1325
66A-VB-PS, 0.5%	56	1350 (0)	107	27.9	1321
66A-VB-PS, 1%	59	1240 (0)	104	28.0	1226
66A-VB-PS, 3%	54	1147 (4)	97	25.9	1340
66A-VB-PS, 5%	53	888 (26)	100	21.1	1394
66B-10A-PS, 0.1%	56	1027 (14)	66	31.9	776
66B-10A-PS, 0.5%	50	1093 (9)	76	32.8	950
66B-10A-PS, 1%	40	972 (19)	75	30.3	936
66B-10A-PS, 3%	32	679 (43)	64	22.9	1025
66B-10A-PS, 5%	44	598 (50)	62	22.2	1104
66B-VB-PS, 0.1%	58	1361 (0)	92	31.0	1092
66B-VB-PS, 0.5%	50	1329 (0)	85	31.0	1151
66B-VB-PS, 1%	56	1337 (0)	99	34.0	1134
66B-VB-PS, 3%	47	1237 (0)	94	29.0	1214
66B-VB-PS, 5%	41	547 (54)	59	21.8	1157
66G-10A-PS, 0.1%	58	1587(0)	126	29.7	1319
66G-10A-PS, 0.5%	55	1481 (0)	132	26.7	1419
66G-10A-PS, 1%	48	1338 (0)	123	24.0	1496
66G-10A-PS, 3%	51	1242 (0)	120	24.1	1458
66G-VB-PS, 0.1%	54	1015 (15)	57	32.9	776
66G-VB-PS, 0.5%	43	926 (23)	62	31.2	825
66G-VB-PS, 1%	50	947 (21)	65	31.9	802
66G-VB-PS, 3%	41	894 (26)	66	30.7	849

Glossary: t_i: time to ignition; THR: total heat released; WLR: mass loss rate; SEA_{av}: Average specific extinction area.

When the data are examined from the point of view of the iron content, it is possible to suggest that, as the iron content increases, the PHRR also increases. This is not in accord with work with montmorillonite, in which there is an iron effect at low amounts of clay but when the amount of clay is 3% or larger, the PHRR is unaffected by the iron content.

One can summarize the cone calorimetry results for various clay-polystyrene nanocomposites as follows: montmorillonite gives a 50–60% reduction in PHRR at 3% clay;[23] while magadiite[12] and fluorohectorite[27] give no reduction and hectorite gives a reduction of up to 50%, but only at 5% clay; the reduction with hectorite at 3% clay is lower than is seen for montmorillonite at this clay level. These variations require an explanation. TEM information is available for all systems and there is excellent dispersion for montmorillonite,

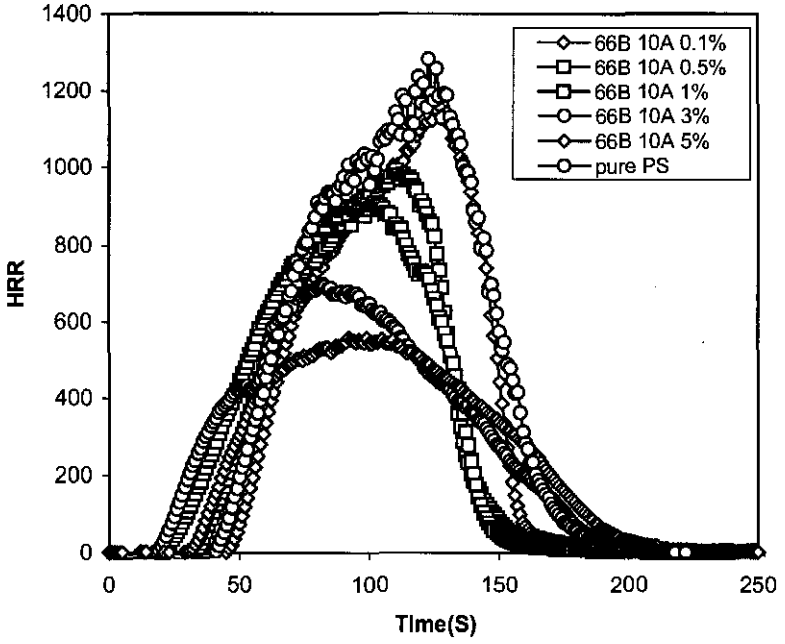

Figure 6 *Heat release rates for the 66B-10A-hectorite-polystyrene nanocomposites*

fluorohectorite and hectorite, but there is some question on the dispersion for magadiite. From previous work in this and other laboratories, there is a correlation between nano-dispersion and reduction in PHRR; good nanodispersion leads to significant reduction in PHRR while no reduction is seen if the clay is not well dispersed.[25,28] For magadiite, the dispersion is not as good as one might like but the enhanced mechanical properties are suggestive of good dispersion. There is a potential sampling problem with TEM in that the amount of material examined is quite small and may not be representative of the whole sample.

We hope to use this information to begin to identify what is important in a clay for fire retardancy. To that end, we must begin by identifying the differences between these various clays; differences that are under consideration include: composition, morphology, charge location, and size. Montmorillonite is an aluminosilicate material while fluorohectorite, hectorite and magadiite are all-silicate materials; since the all silicates give different results, one cannot attribute the differences in PHRR changes to composition.

Previous work showed that there is no difference in PHRR of styrene-montmorillonite nanocomposites for intercalated and exfoliated systems; thus we tentatively decide that changes in morphology, as long as there is good nano-dispersion, do not influence the reduction in PHRR.

Clays consist of octahedral and tetrahedral layers and the substitution of one ion for another may occur in either layer. Differences in charge location might be important, but this information for the clays that have been used is not available and thus cannot be evaluated.

The last difference that has been considered is size. Hectorite is lath-like, while fluorohectorite is much more floppy and tends to fold onto itself to reduce the aspect ratio, and magadiite is very monolithic. The plate diameter and aspect ratios of the clays under consideration are: magadiite, plate diameter ~40 μm, (this is an average reported value obtained from scanning electron microscopy);[30] fluorohectorite, plate diameter, ~4–5 μm,[27] 5 μm,[30] aspect ratio, 500:1 to 4000:1;[27] montmorillonite, plate diameter, ~0.1–1 μm,[27] 0.3–0.6 μm,[30] 0.25 μm,[31] aspect ratio, 100:1 to 1000:1;[27] hectorite, 0.05 μm,[31] ~0.02–0.03 μm.[32] Clearly, there is a great variation in the sizes of the clay particles and it is possible that the differences may be attributed to changes in size. Figure 7 shows plot of the size parameter, peak heat release rate and mass loss rate.

The most accepted process by which the heat release rate is affected by nanocomposite formation is barrier formation.[27] This may occur by loss of the polymer due to thermal degradation so that the clay platelets fall over and come into contact. If the platelet is too large, it may not fall flat but may stick up, leaving a gap in the barrier. However, if the particles are too small, it may require more material to form this impermanent barrier, so the poorer barrier will lead to a smaller reduction in PHRR; this suggests that magadiite and fluorohectorite are too large and do not form a suitable barrier while hectorite, the smallest material, requires additional material to permit the complete reduction in PHRR. One may ask if the larger clays would form a good barrier at higher amounts, which could lead to a substantial reduction in PHRR; this is under investigation.

9.4 Conclusions

Hectorite has been organically-modified with two different ammonium salts and these salts show the same behavior seen with montmorillonite; with an

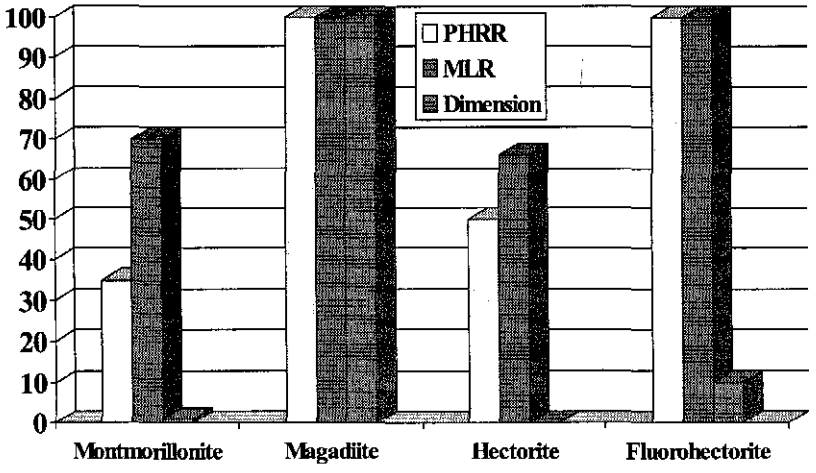

Figure 7 *Comparison of peak heat release rate (PHRR), mass loss rate (MLR), and the dimension of the clay for four different polystyrene-clay nanocomposites*

ammonium salt that contains a styryl unit, exfoliation is observed. When this polymerizable unit is absent, the result is intercalation. Hectorite appears to offer similar thermal properties to montmorillonite but at higher amounts of clay. The significant differences between various clays have been tentatively attributed to differences in size. This is only a tentative conclusion and further work is underway to further elucidate the reason for the differences. Based on this and other work from this laboratory and others, it seems that nanocomposite formation alone will never lead to fire retardancy. Instead, it is felt that nanocomposite formation may be one part of a combination of materials that can be used to achieve fire retardation. The role of the clay is likely to change the heat release rate curve but, more importantly, it will help achieve excellent mechanical properties that may be compromised by the addition of other components of the fire retardancy package. The choice of the clay will probably be made on the basis of enhanced mechanical properties rather than because of some inherent fire retardant properties. Further work is underway to evaluate additional clays and combinations of clays with conventional fire retardants.

9.5 Acknowledgement

This work was performed under the sponsorship of the US Department of Commence, National Institute of Standards and Technology, Grant Number 70NANB6D0119.

9.6 References

1. M. Alexandre and P. Dubois, *Mater. Sci. Eng.*, 2000, **R28**, 1.
2. E.P. Giannelis, R. Krishnamoorti and E. Manias, *Adv. Polym. Sci.*, 1999, **138**, 107.
3. E.P. Giannelis, *Adv. Mater.*, 1996, **8**, 29.
4. R.A. Vaia, K.D. Jandt, E.J. Kramer and E.P. Giannelis, *Chem. Mater.*, 1996, **8**, 2628.
5. D.A. Brune and J. Bicerano, *Polymer*, 2002, **42**, 369.
6. R.K. Bharadwaj, *Macromolecules*, 2001, **34**, 9189.
7. G. Lagaly, K. Beneke and A.Weiss, *Am. Mineral.*, 1975, **60**, 642.
8. K. Beneke and G. Lagaly, *Am. Mineral.*, 1977, **62**, 763.
9. K. Beneke and G. Lagaly, *Am. Mineral.*, 1983, **68**, 818.
10. Y. Sugahara, K. Sugimoto, T. Yanagisawa, Y. Nomizu, K. Kuroda and D. Kato, *Yogyo Kyokai Shi*, 1987, **95**, 117.
11. Z. Wang, T. Lan and T.J. Pinnavaia, *Chem. Mater.*, 1996, **8**, 2200.
12. D. Wang, D.D. Jiang, J. Pabst, Z. Han, J. Wang, and C.A. Wilkie, *Polym. Eng. Sci.*, 2004, **44**, 1122.
13. D. Garcia-Lopez, O. Picazo, J.C. Merino and J.M. Pastor, *Eur. Polym. J.*, 2003, **39**, 945.
14. C. Decker, K. Zahouily, L. Keller, S. Benfarhi, T. Bendaikha and J. Baron, *J. Mater. Sci.*, 2002, **37**, 4831.

15. X. Tong, H. Zhao, T. Tang, Z. Feng and B. Huang, *J Polym. Sci.: Part A: Polym. Chem.*, 2002, **40**, 1706.
16. Z. Shen, G.P. Simon and Y-B. Cheng, *Polymer*, 2002, **43**, 4251.
17. P. Dubois, M. Alexandre, and R. Jerome, *Macromolecular Symposia* (Eurofillers'01 Conference, 2001), 2003, **194**, 13.
18. G. Sandi, K.A. Carrado, H. Joachin, W. Lu and J. Prakash, *J. Power Sources*, 2003, **119–121**, 492.
19. D.W. Kim, A. Blumstein, J. Kumar and S.K. Tripathy, *Polym. Mater. Sci. Eng.*, 2001, **84**,182.
20. S-S. Hou and K.Schmidt-Rohr, *Chem. Mater.*, 2003, **15**, 1938.
21. S-S. Hou, T.J. Bonagamba, F.L. Beyer, P.H. Madison and K. Schmidt-Rohr, *Macromolecules*, 2003, **36**, 2769.
22. G. Sandi, H. Joachin, R. Kizilel, S. Seifert and K.A. Carrado, *Chem. Mater.*, 2003, **15**, 838.
23. J. Zhu, A.B. Morgan, F.J. Lamelas and C.A. Wilkie, *Chem. Mater.*, 2001, **13**, 3774.
24. D. Wang, J. Zhu, Q. Yao and C.A. Wilkie, *Chem. Mater.*, 2002, **14**, 3837.
25. J.W. Gilman, T. Kashiwagi, M. Nyden, J.E.T. Brown, C.L. Jackson and S. Lomakin, in *Chemistry and Technology of Polymer Additives*, S. Al-Maliaka, A. Golovoy and C.A. Wilkie (eds.), Blackwell Scientific, London, 1998, pp. 249–65.
26. J. Zhu, F.M. Uhl, A.B. Morgan and C.A. Wilkie, *Chem. Mater.*, 2001, **13**, 4649.
27. J.W. Gilman, C.L. Jackson, A.B. Morgan, R. Harris, Jr., E. Manias, E.P. Giannelis, M. Wuthenow, D. Hilton and S.H. Phillips, *Chem. Mater.*, 2000, **12**, 1866.
28. D. Wang, D.D. Jiang, J. Pabst and C.A. Wilkie, 2004, **10**, 44.
29. S. Su, D.D. Jiang and C.A. Wilkie, *J. Vinyl Add. Technol.*, in press.
30. J.S. Dailey and T.J. Pinnavaia, *Chem. Mater.*, 1992, **4**, 855.
H.O. Pastore, M. Munsignatti and A.J.S. Mascarenhas, *Clay Clay Miner.*, 2000, **48**, 224. K. Isoda, K. Kuroda and M. Ogawa, *Chem. Mater.*, 2000, **12**, 1702. K. Kikuta, K. Ohta and K. Takagi, *Chem. Mater.*, 2002, **14**, 3123.
31. J. Ren, B.F. Casanueva, C.A. Mitchell and R. Krishnamoorti, *Macromolecules*, 2003, **36**, 4188.
32. S.-S. Hou and K. Schmidt-Rohr, *Chem. Mater.*, 2003, **15**, 1938.
33. T. Kasawa, T. Murakami, N. Kohyama and T. Watanabe, *Am. Mineral.*, 2001, **86**, 105.